International Journal of Applied Science and Mathematics
Volume 2, Issue 4, ISSN (Online): 2394-2894

Synthesis, Phase Formation between Solid Solutions and Photoluminescence Studies on Rare Earth Doped - Glaserite Type Orthovanadate $Ca_9Y_{(1-x)-y}Eu_x[VO_4]_7 : La_y$

A. Duke John David
Voorhees College,
Vellore – Tamil Nadu, India

G. Shakil Muhammad
Islamiah College,
Vaniyambadi – Tamil Nadu, India

V. Sivakumar
National Institute of Technology (NIT) –
Rourkela, India

Abstract **– A new type of orthovanadate $Ca_9Y_{(1-x)-y}Eu_x[VO_4]_7 : La_y$ (x = 0.05 and y = 0 to 1 insteps of 0.2) phosphor was synthesized via the conventional high temperature solid state reaction method. The phase purity and phase transition were studied systematically by Powder X-ray diffraction (PXRD). The PXRD pattern reveals that the synthesized phosphors have a unique crystal structure, which is a rhombhohedral crystal with a slight different lattice paramaters between the two solid solutions. The morphology and elemental analysis of the synthesized compounds was measured by FESEM with EDAX. The diffuse reflectance spectra were measured for all the compositions and the corresponding band gap was calculated. The photoluminescence (PL) study shows a dominant electric dipole and a weak magnetic dipole transitions were observed. The efficient energy transfer from host $[VO_4]$ to Eu^{3+} is confirmed by the PL life time studies. The chromaticity colour coordinate value for this phosphor material is calculated by using emission data and the obtained CIE color coordinate values are very much closer to the NTSC standard values for red colour. This phosphor material can find potential application as a red phosphor for white light emitting diodes.**

Keywords **– A. Phase Formation, B. Solid Solutions, C. Phosphor Material, D. White LEDs.**

I. Introduction

Phosphor research is gaining more attention due to its demand in energy saving and environment friendly characteristics. It is search for a new luminescent materials suitable for solid state lighting and the high resolution display devices. Recently, rare earth doped phosphors have been intensively studied for application such as flat panel displays (FPDs), plasma display panels (PDPs), field emission displays (FEDs) and white light emitting diodes (wLEDs) [1–3]. The luminescence in an inorganic phosphors are composed of a host lattice doped with a small amount of activator ions that activate luminescence. Most of these materials are oxides, sulphides, fluorides, halides, and oxysulphides doped with transition metal ions or rare-earth ions [4]. In recent years the vanadate luminescent materials have been applied to various types of high resolution display systems [5-8]. The vanadate group, namely, $[VO_4]^{3-}$ where the central metal ion V^{5+} is coordinated by four oxygen ligands in a tetragonal symmetry, has broad and intense CT absorption bands (named as O–V CT) in the UV region and some of them can produce broad CT emission spectra from 400 to more than 700 nm related to the local structure [9], [10]. Hence, this typical broadband absorption and emission characteristics makes them suitable for phosphor-converted LEDs.

The activator is the key factor in obtaining efficient emissions in visible spectrum. The trivalent europium ion (Eu^{3+}) is most widely used as an activator in lighting and display fields. It is well-known that the Eu^{3+} emits both orange and red photoluminescence (PL) from f-f transitions ($^5D_0 \rightarrow {}^7F_1$ and $^5D_0 \rightarrow {}^7F_2$), however the intensity depends on the local site symmetry of Eu^{3+}. Eu^{3+} has a simple electronic energy level scheme and its transitions are hypersensitive, i.e., they depend strongly on the chemical surroundings [11].

Rare earth ion-doped vanadates as luminescence materials have been drew much more attention due to the rich color, high luminescence efficiencies, and excellent chemical stabilities. The CT energy generally can be transferred efficiently to the rare earth ions, such as YVO_4:Eu [14], $Ca_9Y(VO_4)_7$:Eu [15], and $Ca_9Y(VO_4)_7$: Tb, Eu [16] and so on.

In the present investigation, we have chosen a phosphor material as $Ca_9Y_{(1-x)-y}Eu_x[VO_4]_7 : La_y$, which comprises of two host lattices i.e., $Ca_9Y(VO_4)_7$ and $Ca_9La(VO_4)_7$, keeping the activator Eu^{3+} constant with 0.05 and varying the La^{3+} for different concentration from 0 to 1 in steps of 0.2. The trivalent rare earth ions Eu^{3+} and La^{3+} were expected to be incorporated into the Y^{3+} in the host lattice, because Y^{3+} ion serves suitable site for trivalent rare earth ion in terms of ionic radius, valence, and optical property. The research work has been carried out to find the structural correlation and photoluminescence properties between these two host lattices in the synthesized phosphor material. The $Ca_9Y_{(1-x)-y}Eu_x[VO_4]_7 : La_y$ phosphor material may be considered as a potential candidate for phosphor pumped by the near UV/blue LED. In addition, this phosphor has good thermal stability since they are synthesized at 800°C for 10 hours.

II. Experimental Section

A. Materials and Synthesis

The new type orthovanadate $Ca_9Y_{(1-x)-y}Eu_x[VO_4]_7 : La_y$ was synthesized via the conventional high temperature solid state reaction method. The high-purity (99.99%, Aldrich) oxides and carbonates were used as precursor and it was a mixture of reagent grade $CaCO_3$, Y_2O_3, La_2O_3, Eu_2O_3 and NH_4VO_3. For the present study, excluding the undoped samples $Ca_9Y[VO_4]$ and $Ca_9La[VO_4]$, we fixed the amount of dopant europium at x = 0.05. The chemicals in the following compositions were taken in

powder form. The concentrations of La^{3+} is varied from 0 to 1 insteps of 0.2. The corresponding precursors are weighed according to the stoichiometric ratio. Each mixture of starting materials is ground for an hour, loaded into a high purity alumina crucible, and then sintered using muffle furnace. First, the stoichiometric mixture was slowly heated up to 350°C for a duration of 7 hours and was kept constant at this temperature for a duration of 5 hours. The obtained powder was mixed again and then heated up to 700°C for 5 hours. The sample was then thoroughly mixed and heated again at a temperature of 780−800°C for 10 hours and cooled down to room temperature to obtain white powder. The obtained synthesized phosphor powder is characterized for its structural phase formation and optical properties.

B. Characterization methods

The Phase purity was checked by powder X-ray diffraction (XRD) analysis collected on a X'Pert PRO analytical diffractometer (45kV, 30mA), using Cu-Kα radiation (λ = 1.5406 Å). The PL excitation and emission spectra of the samples were recorded using a Horiba Jobin Yvon Fluoromax-4 Spectrofluorometer equipped with a 150 W Xe lamp as the excitation source. The surface morphology and elemental analysis is made with FESEM with EDAX instrument by high resolution imaging through CARL ZEISS SUPRA – Oxford Instrument. For the measurements of luminescence decay curves, the Spectroflourometer – Flouorolog- FL3-11 is used. All the measurements were observed at room temperature. The CIE chromaticity coordinates calculated using MATLAB software and CIE calculator – software based system is employed.

III. Results and Discussion

A. Phase formation and structural analysis– [XRD]

The powder X- ray diffraction (pXRD) was carried out for the synthesized powder samples, in order to reveal the phase purity at room temperature. The XRD patterns of annealed phosphor compound $Ca_9Y_{(1-x)-y}Eu_x[VO_4]_2 : La_y$ for various concentrations (x = 0.05 and y = 0 to 0.95 in steps of 0.2) is shown in Fig-1.

The powder X- ray diffraction (pXRD) was carried out for the synthesized powder samples, in order to reveal the phase purity at room temperature. The XRD patterns of annealed phosphor compound $Ca_9Y_{(1-x)-y}Eu_x[VO_4]_2 : La_y$ for various concentrations (x = 0.05 and y = 0 to 0.95 in steps of 0.2) is shown in Fig-1.

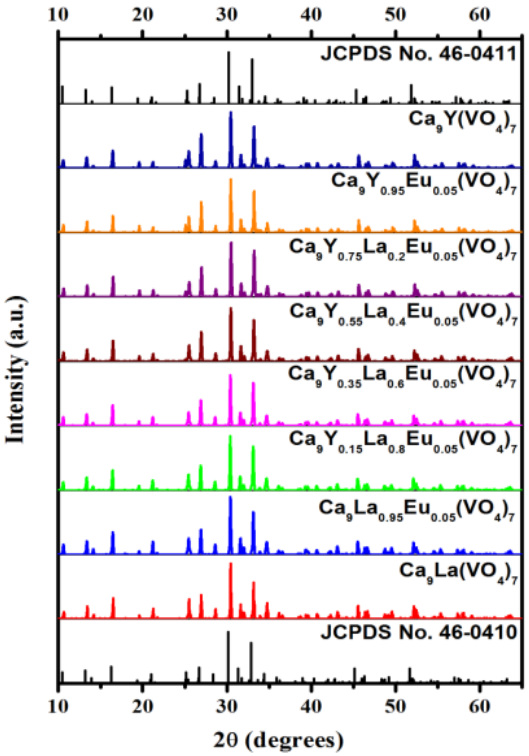

Fig.1. XRD patterns of $Ca_9Y_{(1-x)-y}Eu_x[VO_4]_7 : La_y$ and the standard data cards JCPDS No.46-041 for $Ca_9Y[VO_4]_7$ at the top and JCPDS No.46-0410 for $Ca_9La[VO_4]_7$ bottom.

All the diffraction patterns are well indexed, crystallizes in Rhombohedral structure with a small difference in lattice parameters and no other impurity phases were observed, indicating that single phase was formed and doping the rare earth ions does not cause any significant change in the host lattice structure. The unit cell parameters are listed in the table-1 for the synthesized phosphor material. The activator Eu^{3+} and the La^{3+} substitution in the host lattice doesn't show any change in the crystal structure. It is highly expected that the activator Eu^{3+} and the La^{3+} ions were substituted into host lattice by replacing Y^{3+} ions based on their similar ionic radii. The ionic radius of Eu^{3+} ion is 95 pm and La^{3+} ion is 106 pm, and the host matrix has the lanthanide ion Y^{3+}, which has the ionic radius of 88 pm [17]. This suggests that the Eu^{3+}, La^{3+} ions can easily integrate with the host lattice due to the similarity in the ionic radius. Hence, the pXRD patterns reveal a good and single phase formation between two solid solutions.

Table 1: cell parameters of $Ca_9Y_{(1-x)-y}Eu_x[VO_4]_2: La_y$

Sample	JCPDS No.	a = b / Å	c /Å	V/Å^3	α = β (°)	γ (°)	Space Group
$Ca_9Y(VO_4)_7$	46-0411	10.85	37.98	4477.93	90	120	R3c (161)
$Ca_9La(VO_4)_7$	46-0410	10.89	38.13	4525.84	90	120	R3c (161)

The average crystallite size, D was calculated using the Debye-Scherrer's formula i.e., $D = k\lambda / \beta\cos\theta$, Where β is the full-width at half-maximum (FWHM) of the corresponding XRD peat at radiant, k- the so-called shape factor, which usually takes a value of about ~0.9. λ - is X-ray wavelength ($\lambda_{CuK\alpha}$ = 0.15406 nm) and θ is the Bragg diffraction angle. The average crystallite size of the synthesized phosphor material is found to be 1.14nm. It has been reported that the fine grain size could enhance the emission efficiency and intensity of phosphors [18].

International Journal of Applied Science and Mathematics
Volume 2, Issue 4, ISSN (Online): 2394-2894

B. Morphology and Elemental analysis – [FESEM – EDX]

The host lattice, activator concentrations and also the annealing temperatures plays a key role in the morphology of the phosphor materials. The morphology of the powder particles such as grain size, shape, crystallinity, defects, grain boundary and so on, determines the luminescence efficiency of a phosphor material [19].

The morphology of the synthesized phosphor materials after calcination at 800°C was examined by FESEM and its images are shown in Fig-2 (a to d). The undoped phosphor materials $Ca_9Y(VO_4)_7$ and $Ca_9La(VO_4)_7$ is shown in Fig-2(a&d) respectively. These two undoped images consisted of agglomerated irregular particles, although a type of boundary between the microcrystals can be seen. Fig-2(c&d) shows FESEM images of $Ca_9Y_{0.95}Eu_{0.05}[VO_4]_2$ and $Ca_9La_{0.95}Eu_{0.05}[VO_4]_2$ and the size of these Eu^{3+} activated phosphor materials is in the range of 10 to 100nm.

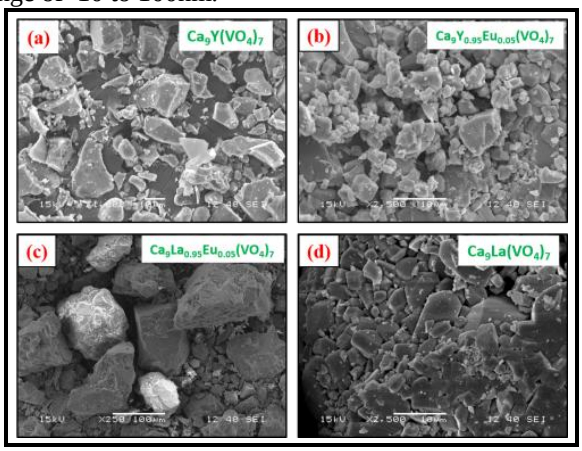

Fig.2. FESEM images $Ca_9Y_{(1-x)-y}Eu_x[VO_4]_7$: La_y; a) $Ca_9Y(VO_4)_7$; b)$Ca_9Y_{0.95}Eu_{0.05}(VO_4)_7$; c) $Ca_9La_{0.95}Eu_{0.05}(VO_4)_7$ and d) $Ca_9La(VO_4)_7$.

It is pointed out earlier that fine crystallite size will enhance the luminescence efficiency of phosphor material. The overview image shows that the particles are separated and clusters were seen. But, it is evident from figure that the particles are in the micrometer range. It is mentioned that crystalline powders and micrometer dimension of the powder with a high strength could be useful for applications, as these micro crystalline phosphors can result in high luminescent intensities [20]. The facts mentioned are all beneficial for the enhancement of photoluminescence property.

The presence of the elements in the synthesized phosphor material was confirmed by the elemental analysis by FESEM with EDX spectroscopy by measuring at different sites of the samples. Fig-3(a & b) shows the EDX spectra for $Ca_9Y_{0.95}Eu_{0.05}[VO_4]_2$ and $Ca_9La_{0.95}Eu_{0.05}[VO_4]_2$ for the selective area inside a square region in the FESEM image.

The EDX spectra, confirms the presence of the existing elements like Calcium (Ca), Yttrium (Y), Vanadium (V), Oxygen (O) and Europium (Eu) as shown in Fig-3(a) and the elements such as Calcium (Ca), Lanthanum (La), Vanadium (V), Oxygen (O) and Europium (Eu) as shown in Fig-3(b) of the synthesized phosphor material.

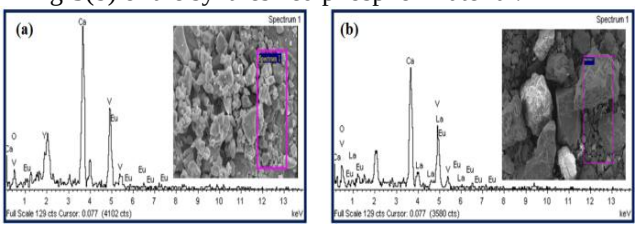

Fig.3. EDX spectra of (a) $Ca_9Y_{0.95}Eu_{0.05}[VO_4]_2$ and (b) $Ca_9La_{0.95}Eu_{0.05}[VO_4]_2$.

C. Diffuse Reflectance Spectroscopy – [UV DRS]

In order to find the optical absorption, transmittance and to calculate the band gap of the synthesized phosphors $Ca_9Y_{(1-x)-y}Eu_x[VO_4]_7$:Lay, the diffuse reflectance spectra were carried out in the range of wavelength from 200 to 800nm. The DRS and the band gap of the undoped phosphor materials $Ca_9Y[VO_4]_7$ and $Ca_9La[VO_4]_7$ is shown in Fig-4(a). The highest percentage of reflectance is observed in the wavelength ranging from 450 to 800nm. It shows a remarkable drop from 450 to 340nm, which corresponds to the band transition and a strong absorption in the range from 340 to 240nm for $Ca_9Y[VO_4]_7$.

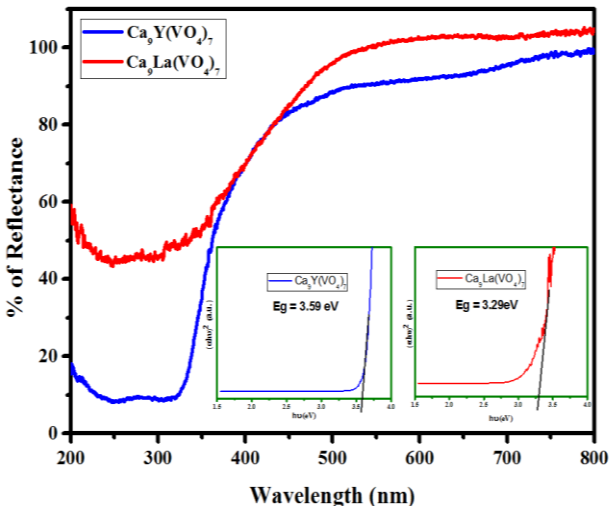

Fig.4. (a): shows diffuse reflectance spectra of undoped $Ca_9Y(VO_4)_7$ and $Ca_9La[VO_4]_7$, the inset shows the band gap plot between $(\alpha h\upsilon)^2$ vs $h\upsilon$

For the phosphor material $Ca_9La[VO_4]_7$, the status of high reflection in the wavelength ranging from 490 to 800nm and then shows a gradual drop from 490 to 350nm, which corresponds to the band transition. A strong absorption is observed from 350 to 250nm.

Broad absorption bands positioned well below 350 nm for the both undoped phosphor materials are associated with the absorption of vanadate groups $[VO_4]^{3-}$ i.e., due to CT transition from oxygen to Vanadate (O-V). A few reports has been made on the complexes of transition metal ions with an empty d – shell often show intense broad band emission with a large Stokes shift. This is generally called as 'ligand to metal charge transfer'(LMCT) transitions (Examples vanadates (VO_4), niobates (NbO_4) and tungstates (WO_4), molybdates (MoO_4) etc.,) [21]. In the present study, the valance band is mainly due to O (2p) orbitals and the conduction band is

made up of V (5d) orbitals. By the absorption of the incident photon, the electron is promoted from the valance band to conduction band.

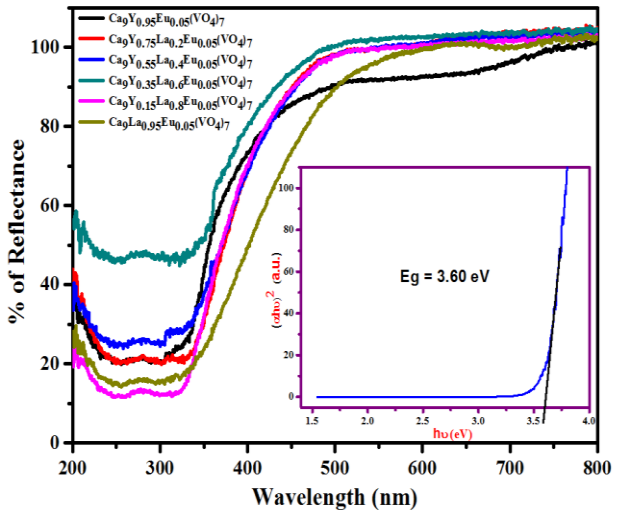

Fig.4. (b): shows diffuse reflectance spectra of $Ca_9Y_{(1-x)-y}Eu_x[VO_4]_7$: La_y with x = 0.05 and y = 0 to 1 insteps of 0.2, the inset shows the band gap plot between $(\alpha h\upsilon)^2$vs hυ

The DRS of $Ca_9Y_{(1-x)-y}Eu_x[VO_4]_7$: La_y with x = 0.05 and y = 0 to 1.0 insteps of 0.2 is shown in Fig-4(b). The highest percentage of reflectance for all the composition as shown in Fig-4(b) is observed in the wavelength range 450 to 800nm. It was found that all the Eu^{3+} and La^{3+} doped compositions shows a strong absorption in the blue to near UV region (240 to 450nm), which is highly essential region for the LED application.

The band gap energies of the direct transition semiconductor can be calculated by a plot of $(\alpha h\upsilon)^2$ Vs. the photon energy (hυ). The absorption coefficient α and direct band gap Eg of synthesized compound can be found by the following equation [22].

$$\alpha h\upsilon = A (h\upsilon - Eg)^{n/2} \quad (1)$$

where α, υ, Eg and A are absorption coefficient, light frequency, the band-gap energy and a constant respectively. The value of the band gap has been determined by extra-plotting the straight line portion of the $(\alpha h\upsilon)^2$ versus hυ graph, which is shown in the inset of Fig-4(b). Thus, the band gap of the as-prepared phosphor materials are calculated and tabulated in table-2.

Table 2: The band gap values $Ca_9Y_{(1-x)-y}Eu_x[VO_4]_7$: La_y

Compound with compositions	**Band gap Eg (eV)**
$Ca_9Y[VO_4]_7$	3.59
$Ca_9Y_{0.95}Eu_{0.05}[VO_4]_7$	3.60
$Ca_9Y_{0.75}Eu_{0.05}[VO_4]_7$: $La_{0.2}$	3.53
$Ca_9Y_{0.55}Eu_{0.05}[VO_4]_7$: $La_{0.4}$	3.42
$Ca_9Y_{0.35}Eu_{0.05}[VO_4]_7$: $La_{0.6}$	3.38
$Ca_9Y_{0.15}Eu_{0.05}[VO_4]_7$: $La_{0.8}$	3.36
$Ca_9La_{0.95}Eu_{0.05}[VO_4]_7$	3.31
$Ca_9La[VO_4]_7$	3.29

D. Photoluminescence properties – [PL]

(i) Photoluminescence properties of $Ca_9Y_{0.95}Eu_{0.05}[VO_4]_7$, excited at λ_{ex} = 392nm.

The excitation spectrum of $Ca_9Y_{0.95}Eu_{0.05}[VO_4]_7$ phosphor material for monitoring the emission at λ_{em} = 612nm is shown in Fig-5(a). The excitation spectrum consists of broad band due to the presence of the vanadate $[VO_4]^{3-}$ and the sharp lines are due to the activator Eu^{3+}. The excitation spectrum exhibits a broadened excitation band from 250 to 350nm with a maximum at about 311 nm, which can be assigned to the overlap of $[VO_4]^{3-}$ excitation and charge transfer transition between Eu^{3+} with empty orbital of $4f^6$ and O^{2-}[23]. Even at 240nm, the excitation intensity is still very strong, which may be assigned to the charge transfer transition between Y^{3+} and O^{2-} at 240nm [24]. The sharp line centered at 392nm results from the $^7F_0$-$^5L_6$ are from the f-f transitions within $4f^n$ configuration of the activator Eu^{3+}.

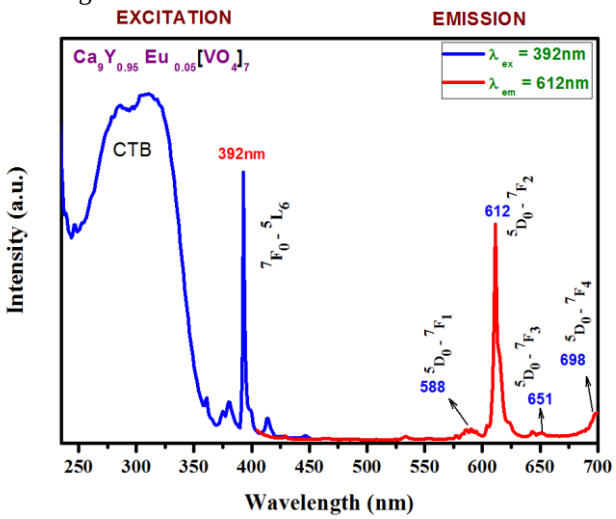

Fig.5. (a): shows photoluminescence excitation and emission spectra of $Ca_9Y_{0.95}Eu_{0.05}[VO_4]_2$

The emission spectrum of $Ca_9Y_{0.95}Eu_{0.05}(VO_4)_7$ is monitored from 400 to 700nm under 392nm near-UV light excitation. The emission spectra consists of several sharp lines from the emission of activator Eu^{3+}, which are associated with the transition from the excited state $^5D_0 \rightarrow {}^7F_J$ (J = 0,1,2,3 and 4). The emission peak at 588nm originates from the magnetic dipole transition $^5D_0 \rightarrow {}^7F_1$. The most intense emission at 612nm results from the electric dipole transition $^5D_0 \rightarrow {}^7F_2$, which is hypersensitive to the environment, i.e. the site symmetry difference of Eu^{3+} ions in different crystal structures results in the difference of the emission spectra. The red light at 612nm closely matches the eye sensitive curves and makes the phosphor ideal for illumination purposes [25]. Also, the emission spectra has weak emission peaks at about 651 and 698nm result from the transitions of $^5D_0 \rightarrow {}^7F_3$ and $^5D_0 \rightarrow {}^7F_4$, respectively, which is not an ideal for illumination.

(ii) Photoluminescence properties of $Ca_9La_{0.95}Eu_{0.05}[VO_4]_7$, excited at λ_{ex} = 392nm.

A similar kind of photoluminescence spectra is observed in $Ca_9La_{0.95}Eu_{0.05}(VO_4)_7$ for monitoring the emission at

λ_{em} = 612nm is shown in Fig-5(b). The excitation spectrum consists of broad band due to the presence of the vanadate $[VO_4]^{3-}$ and the sharp lines are due to the activator Eu^{3+}. The excitation spectrum exhibits a broadened excitation band from 250 to 350nm with a maximum at about 307 nm, which can be assigned to the overlap of $[VO_4]^{3-}$ excitation and charge transfer (CT) transition between Eu^{3+} with empty orbital of $4f^6$ and O^{2-}[23]. Even at 240 nm, the excitation intensity is still very strong, which may be assigned to the charge transfer transition between La^{3+} and O^{2-} at 240nm [24]. The sharp line centered at 392nm results from the $^7F_0$-$^5L_6$ are from the f-f transitions within 4f ^{n} configuration of the activator Eu^{3+}.

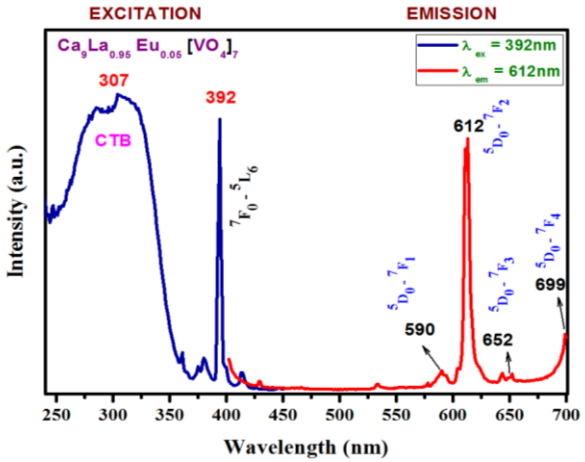

Fig.5. (b) shows photoluminescence excitation and emission spectra of $Ca_9La_{0.95}Eu_{0.05}(VO_4)_7$

The emission spectrum of $Ca_9La_{0.95}Eu_{0.05}(VO_4)_7$ is monitored from 400 to 700nm under 392nm near-UV light excitation. The emission spectra consists of several sharp lines from the emission of activator Eu^{3+}, which are associated with the transition from the excited state to ground state as $^5D_0 \rightarrow {}^7F_J$ (J = 0,1,2,3 and 4). The rest of the emission spectrum is similar to $Ca_9La_{0.95}Eu_{0.05}(VO_4)_7$.

(iii) Photoluminescence [PL] Emission Spectra series of $Ca_9Y_{(1-x)-y}Eu_x[VO_4]_7 : La_y$, excited at λ_{ex} =392 and 465nm.

A 3D-plot of PL emission spectra series of the synthesized phosphor material $Ca_9Y_{(1-x)-y}Eu_x[VO_4]_7 : La_y$ with different concentrations, ranging from x = 0.05 and y = 0 to 1.0 (insteps of 0.2), excited at a wavelength of λ_{ex} =392 and 465nm is shown in Fig-6(a & b). From these plots, one can observe that the highest intensity is at 612nm ascribed to $^5D_0 \rightarrow {}^7F_2$ transitions is dominating, due to the electric dipole transition.

According to the Judd–Ofelt theory, the magnetic dipole transition is permitted. However, the electric dipole transition is allowed only when the europium ion occupies a site without an inversion center and the intensity is significantly affected by the symmetry in local environments around Eu^{3+} ions [26, 27].

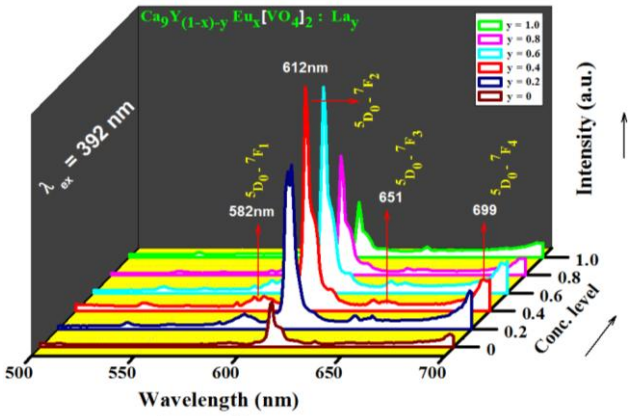

Fig.6. (a) shows 3D plot – PL emission spectra series of $Ca_9Y_{(1-x)-y}Eu_x[VO_4]_7 : La_y$, λ_{ex} = 392nm.

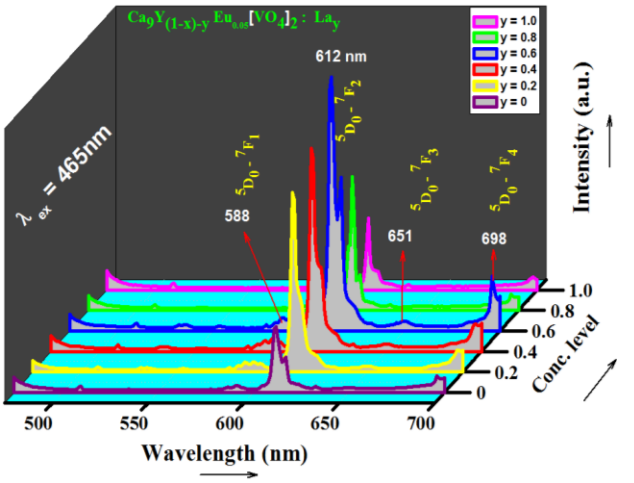

Fig.6. (b) shows 3D plot – PL emission spectra series of $Ca_9La_{(1-x)-y}Eu_x[VO_4]_7 : La_y$, λ_{ex} = 465nm.

If the Eu^{3+} ions occupy an inversion symmetry site, the orange-red emission, magnetic dipole transition $^5D_0 \rightarrow {}^7F_1$ (at 588nm) is the less dominant transition than the electric dipole transition $^5D_0 \rightarrow {}^7F_2$ (at 615nm) [28]. According to these sharp emission lines, it can be concluded that most Eu^{3+} ions have non inversion center and the electric dipole transition $^5D_0 \rightarrow {}^7F_2$ (at 615nm) is dominant. As reported earlier that the La^{3+} and Y^{3+} rich compositions have non-centrosymmetric site. Hence the substitution of Eu^{3+} in La^{3+} and Y^{3+} rich composition show intense red emission (ED). Other transitions from the $^5D_0 \rightarrow {}^7F_1$, $^5D_0 \rightarrow {}^7F_3$ and $^5D_0 \rightarrow {}^7F_4$, were relatively weak. Therefore the f-f transition emission of rare earth ions predominates and the O-V CT emission is very weak due to the efficient energy transfer between the $[VO_4]^{3-}$ to the rare earth ion Eu^{3+}. All the compositions show red emission, however the relative intensity only varies.

D. Life time measurement PL – [Decay curve]

The luminescence lifetime is a key factor for luminescence probe. The fluorescence decay curves of $^5D_0 \rightarrow {}^7F_2$ electric dipole transition of Eu^{3+} at 612 nm under 392nm excitation are measured and shown in Fig-7(a) & (b).

International Journal of Applied Science and Mathematics
Volume 2, Issue 4, ISSN (Online): 2394-2894

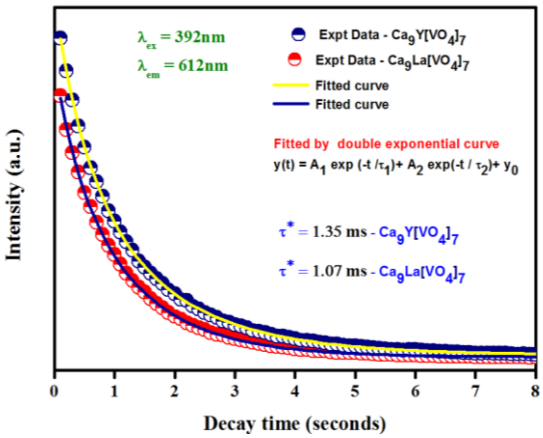

Fig.7. (a) PL decay lifetime measurement for $Ca_9Y[VO_4]_7$ and $Ca_9La[VO_4]_7$

The lifetime decay curves have been analyzed by curve-fitting and all the decay curves for emission of Eu^{3+} can be well-fitted successfully based on the following double-exponential equation (1) [29] revealing the presence of Eu^{3+} environment is unique.

$$y(t) = A_1 \exp(-t/\tau_1) + A_2 \exp(-t/\tau_2) + y_0 \quad \text{------ (1)}$$

Here y(t) is the luminescence intensity at time t after the cut-off of the excitation light. A_1 and A_2 are pre-exponential factors associated with the lifetime components τ_1 and τ_2 respectively. The average lifetime of the synthesized phosphor materials can be calculated by using equation (2) [30].

$$\tau^*_{(avg)} = \frac{A_1\tau_1^2 + A_2\tau_2^2}{A_1\tau_1 + A_2\tau_2} \quad \text{------ (2)}$$

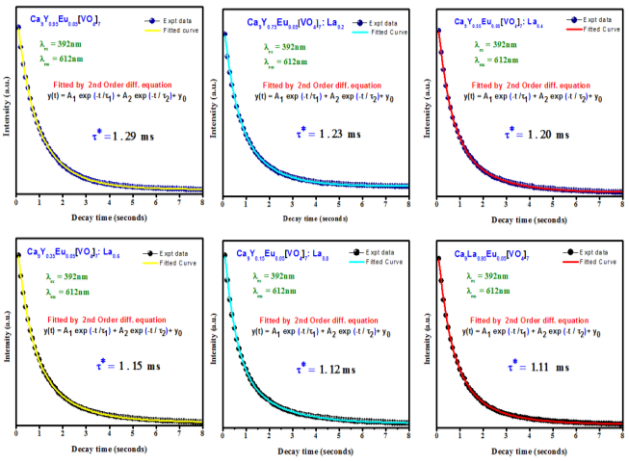

Fig.7. (b) shows PL decay lifetime measurement for series of $Ca_9Y_{(1-x)-y}Eu_x[VO_4]_7 : La_y$, λ_{ex} = 465nm.

The average lifetime of the synthesized phosphor material at λ_{em} =612nm emission, which was estimated at various concentrations, are summarized in Table-3. The 612nm emission due to Eu^{3+} takes a much longer decay time for all of the doped samples. It is noted that the average decay time (τ*) decreases gradually. This behaviour may be attributed to the efficient energy transfer between the vanadate group $[VO_4]^{3-}$ and the dopants Eu^{3+} and other trivalent rare earth ions Y^{3+} and La^{3+} ions.

Table 3: shows the average life time of phosphor material $Ca_9Y_{(1-x)-y}Eu_x[VO_4]_7 : La_y$,

Compound with composition	Avg. lifetime $\tau^*_{avg.}$ (ms)
$Ca_9Y[VO_4]_7$	1.35
$Ca_9Y_{0.95}Eu_{0.05}[VO_4]_7$	1.29
$Ca_9Y_{0.75}Eu_{0.05}[VO_4]_7$: $La_{0.2}$	1.23
$Ca_9Y_{0.55}Eu_{0.05}[VO_4]_7$: $La_{0.4}$	1.20
$Ca_9Y_{0.35}Eu_{0.05}[VO_4]_7$: $La_{0.6}$	1.15
$Ca_9Y_{0.15}Eu_{0.05}[VO_4]_7$: $La_{0.8}$	1.12
$Ca_9La_{0.95}Eu_{0.05}[VO_4]_7$	1.11
$Ca_9La[VO_4]_7$	1.07

E. CIE - Chromaticity Coordinates

The CIE (Commission International del'Eclairage - 1931) chromaticity coordinate value for the $Ca_9Y_{(1-x)-y}Eu_x[VO_4]_7 : La_y$ phosphors excited at 392nm and 465nm were calculated and is indicated by a mark as shown in Fig-8. The CIE plot shown here indicates the undoped compounds $Ca_9Y[VO_4]_7$ and $Ca_9La[VO_4]_7$ as encircled with red colour. And also, it shows the highest intensity only, for the excitation wavelength 392 and 465nm as encircled in green colour show in Figure-8. The CIE chromaticity coordinate values for the host are calculated and it is found to be x = 0.265 and y = 0.387 (green region) for $Ca_9Y[VO_4]_7$ and x = 0.285 and y = 0.353 (green region) for $Ca_9La[VO_4]_7$. The CIE chromaticity coordinate values for the composition $Ca_9Y_{0.55}Eu_{0.05}[VO_4]_7$: $La_{0.4}$ is calculated and found to be x = 0.626 and y = 0.371 (red region), excited at 392nm and for the composition $Ca_9Y_{0.35}Eu_{0.05}[VO_4]_7$: $La_{0.6}$ is calculated, it is found to be x = 0.659 and y = 0.347 (red region), excited at 465nm. This value is very much close to the National Television Standard Committee (NTSC) standard values with (x = 0.670 and y = 0.33) [31]. This indicates that the red light emitted by $Ca_9Y_{0.35}Eu_{0.05}[VO_4]_7$: $La_{0.6}$ is of high color purity. Hence, this red phosphor can find potential application in the white LEDs.

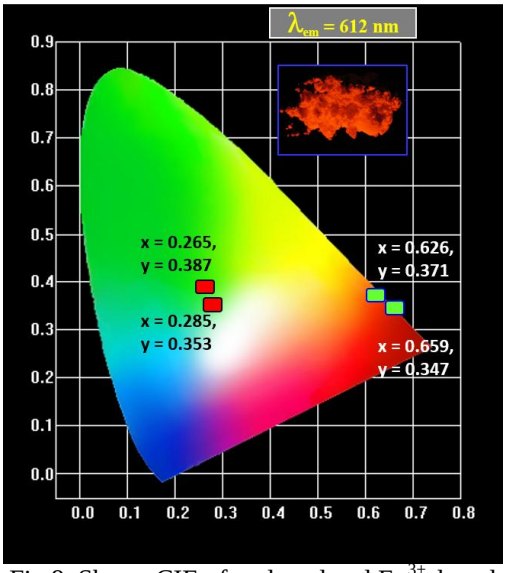

Fig.8. Shows CIE of undoped and Eu^{3+} doped orthovanadate

IV. CONCLUSION

A new phosphor material $Ca_9Y_{(1-x)-y}Eu_x[VO_4]_7$: La_y is successfully synthesized by solid state reaction route. Solid solution between Eu^{3+} activated $Ca_9Y[VO_4]_7$ and $Ca_9La[VO_4]_7$ has been made and studied on their photoluminescence properties. The powder X-ray diffraction patterns shows that there is a unique phase rhombhohedral with slight difference in the unit cell parameters between the two solid solutions. The morphology of the synthesized phosphors have been investigated by FESEM and it shows irregular shape and the size range in micrometres, which influences the photoluminescence property. From the EDX, the presence of the existing elements are confirmed viz., Ca, Y, La, Eu, V and O. Diffuse Reflectance Spectra studies show broad absorption band which is due to charge transfer from O to V in the host lattice. The band gap was calculated from diffuse reflectance spectra and it was found to be 3.43 eV. The Photoluminescence studies show a good excitation spectra from 240 to 400 nm (where the LED emission occurs). The emission spectra shows a dominant electric dipole (ED) transition, however the intensity is dependent on the phosphor compositions. The ED transition is dominant for both the excitation i.e., at λ_{ex} = 392 and 465nm. The life time studies show that there is a slight decrease in life time, which infers an efficient energy transfer from the host lattice to the dopant. The calculated CIE chromaticity color coordinate values are well matched with the NTSC standard value. Hence, this phosphor material can be a potential candidate to be used as red phosphor for the white light emitting diodes.

REFERENCES

[1] F.C. Palilla, A.K. Levine, M. Rinkevics, *J. Electrochem. Soc*. 112 (8) (1965) 776.
[2] K.A. Wickersheim, R.A. Lefever, *J. Electrochem. Soc.* 111 (1) (1964) 47.
[3] R.C. Ropp, *J. Electrochem. Soc.* 111 (3) (1964) 311.
[4] Schnick, W., *Inter. J. Inorg. Mater*., 3, (2001),1267.
[5] Nakajima T, Isobe M, Tsuchiya T, Ueda Y, Manabe T .*J.Phys Chem* 114: (2010);5160–7.
[6] Nakajima T, Isobe M, Tsuchiya T, Ueda Y, Kumagai T. *J. Lumin*129: (2009);1598–601.
[7] Ronde H, Snijder J G.*Chem Phys Lett* 50(1977);282–3.
[8] Huang Y L, YuYM, Tsuboi T, Seo H *J.Opt Exp* 20: (2012); 4360–8.
[9] H. Gobrecht, G. Heinsohn, Zeitschrift für *Physik* 147 (1957) 350.
[10] H. Ronde, G. Blasse, *J. Inorg. Nucl. Chem*. 40 (1978) 215–219.
[11] G. Blasse, A. Bril, W.-C. Nieuwpoort, 27 (1966) 1587–1592.
[12] C. Qin, Y. Huang, H.J. Seo, *J. Am. Ceram. Soc.* 96 (2013) 1181.
[13] X. Wu, Y. Huang, L. Shi, H.J. Seo, *Mater. Chem. Phys*. 116 (2009) 449
[14] D. Wawrzynczyk, M. Nyk, M. Samoc, *J. Mater. Chem.* C 1 (2013) 5837.
[15] S. Cao, Y. Ma, C. Quan, W. Zhu, K. Yang, W. Yin, *J. Alloys Comp*. 487 (2009) 346.
[16] Ling Li, Xiao Guang Liu, Hyeon Mi Noh, *J. Solid State Chem*. 221 (2015) 95–101
[17] R.D. Shannon, Acta Crystallogr. A32 (1976) 751.
[18] W.T. Hsu, W.H. Wu, C.H. Lu, *Mater. Sci. Eng. B* 104 (2003) 40.
[19] Atabaev TS, Vu H-HT, Piao Z, Kim H-K, Hwang Y-H. 541 (2012), 263-268.
[20] X. Xiao, B. Yan, *Mater. Sci. Eng. B* 136 (2007) 154–158.
[21] Blasse, G. and B.C. Grabmaier *Luminescent Materials*, Springer-Verlag, Berlin, 1994.
[22] J.Tau, *Mater. Res. Bull.* 5 (1970) 721-729
[23] Y.L. Huang, W.X. Zhao, Y.G. Cao, Kiwan Jang, *J. Solid State Chem.* 181 (2008) 2161.
[24] J.K. Berkowitz, J.A. Olsen, *J. Lumin*. 50 (1991) 111.
[25] Y. Gautam Gundiah, N. Shimomura, A.K. Kijima, Cheetham, CPLett.455 (2008) 279.
[26] B.R. Judd, *Phys. Rev*. 127 (1962) 750.
[27] G.S. Ofelt, *J. Chem. Phys.* 37 (1962) 511.
[28] G. Blasse, *Chem. Phys. Lett*. 20 (1973) 573–574.
[29] Z.G. Xia, L.B. Liao, Z.P. Zhang, Y.F. Wang, 47 (2012) 405.
[30] Z.G. Xia, X.M. Wang, Y.X. Wang, L.B. Liao, X.P. 50 (2011) 10134.
[31] Koike, J., Kojima, T., Toyonaga, R., Kagami, A., Hase, T., and Inaho,126, (1979), 1008.